

HENRY

Hydraulic Engineering Repository

Ein Service der Bundesanstalt für Wasserbau

Article, Published Version

Schüttrumpf, Holger; Kortenhaus, Andreas; Pullen, Tim; Allsop, William; Bruce, Tom; Meer van der, Jentsje

Prediction of overtopping

Die Küste

Zur Verfügung gestellt in Kooperation mit/Provided in Cooperation with:
Kuratorium für Forschung im Küsteningenieurwesen (KFKI)

Verfügbar unter/Available at: <https://hdl.handle.net/20.500.11970/101584>

Vorgeschlagene Zitierweise/Suggested citation:

Schüttrumpf, Holger; Kortenhaus, Andreas; Pullen, Tim; Allsop, William; Bruce, Tom; Meer van der, Jentsje (2007): Prediction of overtopping. In: Die Küste 73. Heide, Holstein: Boyens. S. 40-68.

Standardnutzungsbedingungen/Terms of Use:

Die Dokumente in HENRY stehen unter der Creative Commons Lizenz CC BY 4.0, sofern keine abweichenden Nutzungsbedingungen getroffen wurden. Damit ist sowohl die kommerzielle Nutzung als auch das Teilen, die Weiterbearbeitung und Speicherung erlaubt. Das Verwenden und das Bearbeiten stehen unter der Bedingung der Namensnennung. Im Einzelfall kann eine restriktivere Lizenz gelten; dann gelten abweichend von den obigen Nutzungsbedingungen die in der dort genannten Lizenz gewährten Nutzungsrechte.

Documents in HENRY are made available under the Creative Commons License CC BY 4.0, if no other license is applicable. Under CC BY 4.0 commercial use and sharing, remixing, transforming, and building upon the material of the work is permitted. In some cases a different, more restrictive license may apply; if applicable the terms of the restrictive license will be binding.



4. Prediction of overtopping

4.1 Introduction

A number of different methods may be available to predict overtopping of particular structures (usually simplified sections) under given wave conditions and water levels. Each method will have strengths or weaknesses in different circumstances. In theory, an analytical method can be used to relate the driving process (waves) and the structure to the response through equations based directly on a knowledge of the physics of the process. It is however extremely rare for the structure, the waves and the overtopping process to all be so simple and well-controlled that an analytical method on its own can give reliable predictions. Analytical methods are not therefore discussed further in this manual.

The primary prediction methods are therefore based on empirical methods (Section 4.2) that relate the overtopping response (usually mean overtopping discharge) to the main wave and structure parameters. Two other methods have been derived during the CLASH European project based on the use of measured overtopping from model tests and field measurements. The first of these techniques uses the CLASH database of structures, waves and overtopping discharges, with each test described by 13 parameters. Using the database (Section 4.5) is however potentially complicated, requiring some familiarity with these type of data. A simpler approach, and much more rapid, is to use the Neural Network tool (Section 4.3) that has been trained using the test results in the database. The Neural Network tool can be run automatically on a computer as a stand-alone device, or embedded within other simulation methods.

For situations for which empirical test data do not already exist, or where the methods above do not give reliable enough results, then two alternative methods may be used, but both are more complicated than the three methods described in Sections 4.2 to 4.5. A range of numerical models can be used to simulate the process of overtopping (Section 4.6). All such models involve some simplification of the overtopping process and are therefore limited to particular types of structure or types of wave exposure. They may however run sequences of waves giving overtopping (or not) on a wave-by-wave basis. Generally, numerical models require more skill and familiarity to run successfully.

The final method discussed here is physical modelling in which a scale model is tested with correctly scaled wave conditions. Typically such models may be built to a geometric scale typically in the range 1:20 to 1:60, see discussion on model and scale effects in Section 4.8. Waves will be generated as random wave trains each conforming to a particular energy spectrum. The model may represent a structure cross-section in a 2-dimensional model tested in a wave flume. Structures with more complex plan shapes, junctions, transitions etc., may be tested in a 3-dimensional model in a wave basin. Physical models can be used to measure many different aspects of overtopping such as wave-by-wave volumes, overtopping velocities and depths, as well as other responses.

4.2 Empirical models, including comparison of structures

4.2.1 Mean overtopping discharge

Empirical methods use a simplified representation of the physics of the process presented in (usually dimensionless) equations to relate the main response parameters (overtop-

ping discharge etc) to key wave and structure parameters. The form and coefficients of the equations are adjusted to reproduce results from physical model (or field) measurements of waves and overtopping.

Empirical equations may be solved explicitly, or may occasionally require iterative methods to solve. Historically some empirical methods have been presented graphically, although this is now very rare.

The mean overtopping discharge, q , is the main parameter in the overtopping process. It is of course not the only parameter, but it is easy to measure in a laboratory wave flume or basin, and most other parameters are related in some way to this overtopping discharge. The overtopping discharge is given in m^3/s per m width and in practical applications often in litres/s per m width. Although it is given as a discharge, the actual process of wave overtopping is much more dynamic. Only large waves will reach the crest of the structure and will overtop with a lot of water in a few seconds. This wave by wave overtopping is more difficult to measure in a laboratory than the mean overtopping discharge.

As the mean overtopping discharge is quite easy to measure many physical model tests have been performed all over the world, both for scientific (idealised) structures and real applications or designs. The European CLASH project resulted in a large database of more than 10,000 wave overtopping tests on all kind of structures (see Section 4.5). Some series of tests have been used to develop empirical methods for prediction of overtopping. Very often the empirical methods or formulae are applicable for typical structures only, like smooth slopes (dikes, sloping seawalls), rubble mound structures or vertical structures (caissons) or walls.

Chapters 5, 6 and 7 will describe in detail formulae for the different kinds of structure. In this section an overall view will be given in order to compare different structures and to give more insight into how wave overtopping behaves for different kind of structures. The structures considered here with governing overtopping equations (more details in Chapters 5, 6 and 7) are: smooth sloping structures (dikes, seawalls); rubble mound structures (breakwaters, rock slopes); and vertical structures (caissons, sheet pile walls).

The principal formula used for wave overtopping is:

$$\frac{q}{\sqrt{gH_{m0}^3}} = a \exp(-bR_c / H_{m0}) \quad 4.1$$

It is an exponential function with the dimensionless overtopping discharge $q/(gH_{m0}^3)^{1/2}$ and the relative crest freeboard R_c/H_{m0} . This type of equation shown in a log-linear graph gives a straight line, which makes it easy to compare the formulae for various structures. Specific equations are given in Chapters 5 and 6 for smooth and rubble mound structures and sometimes include a berm, oblique wave attack, wave walls and the slope angle and wave period or wave steepness.

Two equations are considered for pulsating waves on a vertical structure. ALLSOP et al. (1995) consider relatively shallow water and FRANCO et al. (1994) more deep water (caissons). Vertical structures in shallow water, and often with a sloping foreshore in front, may become subject to impulsive forces, i.e. high impacts and water splashing high up into the air. Specific formulae have been developed for these kinds of situation.

For easy comparison of different structures, like smooth and rubble mound sloping structures and vertical structures for pulsating and impulsive waves, some simplifications will be assumed.

In order to simplify the smooth structure no berm is considered ($\gamma_b = 1$), only perpendicular wave attack is present ($\gamma_\beta = 1$), and no vertical wall on top of the structure is present

($\gamma_v = 1$). As a smooth structure is considered also, $\gamma_f = 1$. This limits the structure to a smooth and straight slope with perpendicular wave attack. The slope angles considered for smooth slopes are $\cot\alpha = 1$ to 8, which means from very steep to very gentle. If relevant a wave steepness of $s_o = 0.04$ (steep storm waves) and 0.01 (long waves due to swell or wave breaking) will be considered.

The same equation as for smooth sloping structures is applicable for rubble mound slopes, but now with a roughness factor of $\gamma_f = 0.5$, simulating a rock structure. Rubble mound structures are often steep, but rock slopes may also be gentle. Therefore slope angles with $\cot\alpha = 1.5$ and 4.0 are considered.

For vertical structures under pulsating waves both formulae of ALLSOP et al. (1995) and FRANCO et al. (1994) will be compared, together with the formula for impulsive waves. Impulsive waves can only be reached with a relatively steep foreshore in front of the vertical wall. For comparison values of the ratio wave height/water depth of $H_{m0}/h_s = 0.5, 0.7$ & 0.9 will be used.

Smooth slopes can be compared with rubble mound slopes and with vertical structures under pulsating or impulsive conditions. First the traditional graph is given in Fig. 4.1 with the relative freeboard R_c/H_{m0} versus the logarithmic dimensionless overtopping $q/(gH_{m0}^3)^{1/2}$.

In most cases the steep smooth slope gives the largest overtopping. Steep means $\cot\alpha < 2$, but also a little gentler if long waves (small steepness) are considered. Under these conditions waves surge up the steep slope. For gentler slopes waves break as plunging waves and this reduces wave overtopping. The gentle slope with $\cot\alpha = 4$ gives much lower overtopping than the steep smooth slopes. Both slope angle and wave period have influence on overtopping for gentle slopes.

The large roughness and high permeability of a rubble mound structures reduces wave overtopping to a greater extent; see Fig. 4.1. A roughness factor of $\gamma_f = 0.5$ was used and a value of 0.4 (two layers of rock on a permeable under layer) would even reduce the overtopping further. The gentle rubble mound slope with $\cot\alpha = 4$ gives very low overtopping.

Vertical structures under pulsating waves (ALLSOP et al., 1995 and FRANCO et al., 1994) give lower overtopping than steep smooth slopes, but more than a rough rubble mound slope. The impulsive conditions give a different trend. First of all, the influence of the relative water depth is fairly small as all curves with different H_{m0}/h_s are quite close. For low vertical structures ($R_c/H_{m0} < 1.5$) there is hardly any difference between pulsating and impulsive conditions. The large difference is present for higher vertical structures and certainly for the very high structures. With impulsive conditions water is thrown high into the air, which means that overtopping occurs even for very high structures. The vertical distance that the discharge travels is more or less independent of the actual height of the structure. For $R_c/H_{m0} > 3$ the curves are almost horizontal.

Another way of comparing various structures is to show the influence of the slope angle on wave overtopping, and this has been done in Fig. 4.2. A vertical structure means $\cot\alpha = 0$. Steep smooth structures can roughly be described by $1 \leq \cot\alpha \leq 3$. Battered walls have $0 < \cot\alpha < 1$. Gentle slopes have roughly $\cot\alpha \geq 2$ or 3. Fig. 4.2 shows curves for two relative freeboards: $R_c/H_{m0} = 1.5$ & 3.0.

Of course similar conclusions can be drawn as for the previous comparison. Steep slopes give the largest overtopping, which reduces for gentler slopes; for a given wave condition and

water level. Vertical slopes give less overtopping than steep smooth slopes, except for a high vertical structure under impulsive conditions.

Details of all equations used here are described in Chapter 5 (sloping smooth structures), Chapter 6 (rubble mound structures) and Chapter 7 (vertical structures).

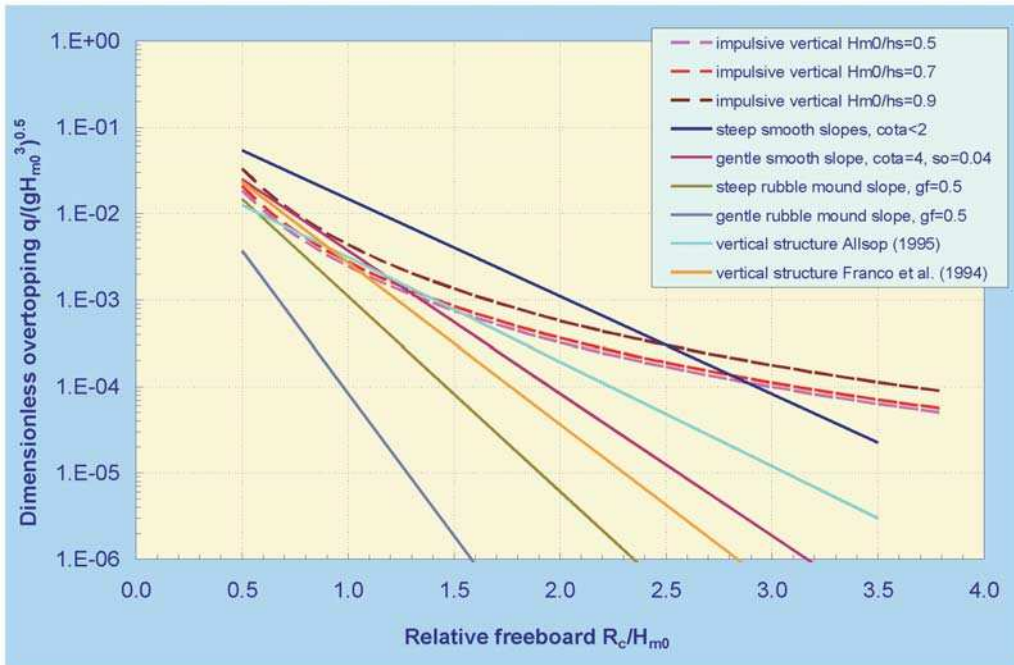


Fig. 4.1: Comparison of wave overtopping formulae for various kind of structures

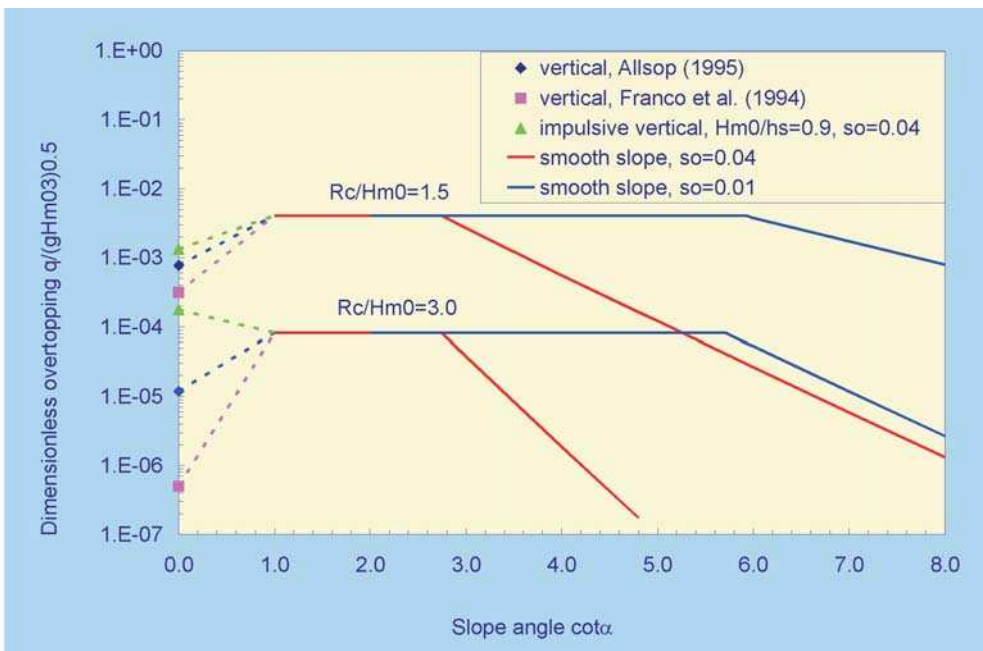


Fig. 4.2: Comparison of wave overtopping as function of slope angle

4.2.2 Overtopping volumes and V_{\max}

Wave overtopping is a dynamic and irregular process and the mean overtopping discharge, q , does not cover this aspect. But by knowing the storm duration, t , and the number of overtopping waves in that period, N_{ow} , it is easy to describe this irregular and dynamic overtopping, if the overtopping discharge, q , is known. Each overtopping wave gives a certain overtopping volume of water, V and this can be given as a distribution

As many equations in this manual, the two-parameter Weibull distribution describes the behaviour quite well. This equation has a shape parameter, b , and a scale parameter, a . The shape parameter gives a lot of information on the type of distribution. Fig. 4.3 gives an overall view of some well-known distributions. The horizontal axis gives the probability of exceedance and has been plotted according to the Rayleigh distribution. The reason for this is that waves at deep water have a Rayleigh distribution and every parameter related to the deep water wave conditions, like shallow water waves or wave overtopping, directly show the deviation from such a Rayleigh distribution in the graph. A Rayleigh distribution should be a straight line in Fig. 4.3 and a deviation from a straight line means a deviation from the Rayleigh distribution.

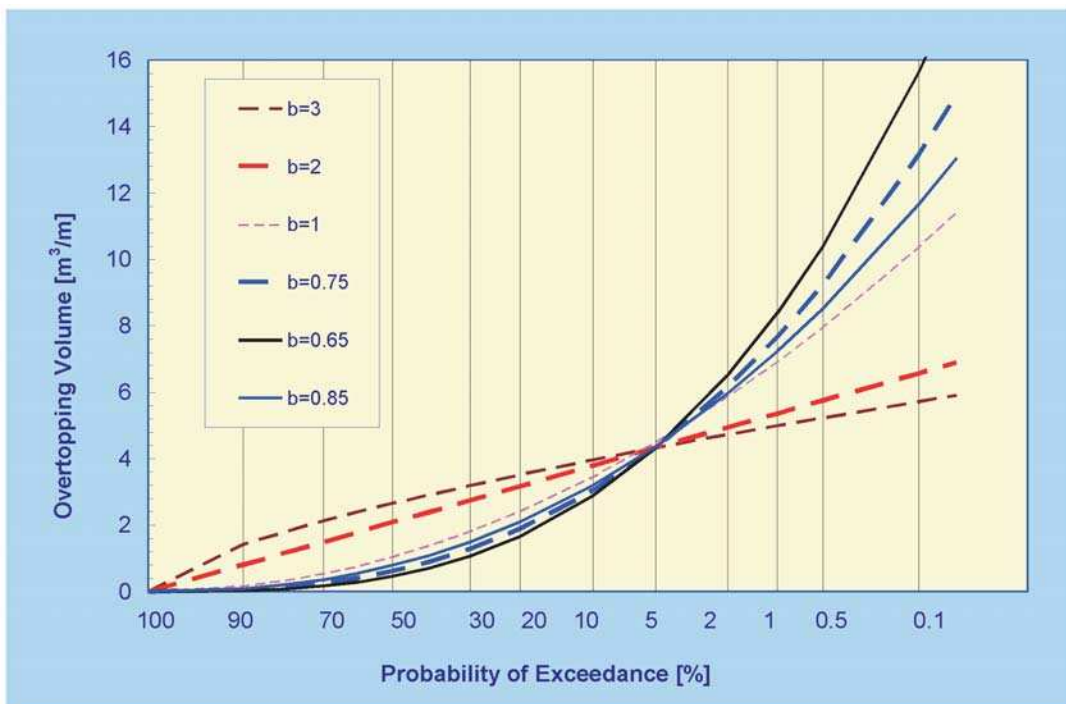


Fig. 4.3: Various distributions on a Rayleigh scale graph. A straight line ($b = 2$) is a Rayleigh distribution

When waves approach shallow water and the highest waves break, the wave distribution turns into a Weibull distribution with $b > 2$; also refer to Fig. 2.5. An example with $b=3$ is shown in Fig. 4.3 and this indicates that there are more large waves of similar height. The exponential distribution (often found for extreme wave climates) has $b = 1$ and shows that extremes become larger compared to most of the data. Such an exponential distribution would give a straight line in a log-linear graph.

The distribution of overtopping volumes for all kind of structures have average values even smaller than $b = 1$. Such a distribution is even steeper than an exponential distribution. It means that the wave overtopping process can be described by a lot of fairly small or limited overtopping volumes and a few very large volumes. The EA-manual (1999) gives various b -values (and according a -values), based on different and limited data sets. The b -values are mostly within the range $0.6 < b < 0.9$. For comparison curves with $b = 0.65$ and 0.85 are given in Fig. 4.3. The curves are very similar, except that the extremes differ a little. It is for this reason that for smooth slopes an average b -value of 0.75 was chosen and not different values for various subsets of data. The same average value has been used for rubble mound structures, which makes smooth and rubble mound structures easy comparable. The exceedance probability, P_v of an overtopping volume per wave is then similar to:

$$P_v = P(\underline{V} \leq V) = 1 - \exp\left[-\left(\frac{V}{a}\right)^{0.75}\right] \quad 4.2$$

with:

$$a = 0.84 \cdot T_m \cdot \frac{q}{P_{ov}} = 0.84 \cdot T_m \cdot q \cdot N_w / N_{ow} = 0.84 \cdot q \cdot t / N_{ow} \quad 4.3$$

Equation 4.3 shows that the scale parameter a , depends on the overtopping discharge, q , but also on the mean period, T_m , and probability of overtopping, N_{ow}/N_w , or which is similar, on the storm duration, t , and the actual number of overtopping waves N_w .

Equations for calculating the overtopping volume per wave for a given probability of exceedance, is given by Equation 4.2. The maximum overtopping during a certain event is fairly uncertain, as most maxima, but depends on the duration of the event. In a 6 hours period one may expect a larger maximum than only during 15 minutes. The maximum overtopping volume by only one wave during an event depends on the actual number of overtopping waves, N_{ow} , and can be calculated by:

$$V_{max} = a \cdot [\ln(N_{ow})]^{4/3} \quad 4.4$$

Chapters 5, 6 and 7 give formulae for smooth slopes, rubble mound slopes and vertical walls, respectively. In this Section and example is given between the mean overtopping discharge, q , and the maximum overtopping volume in the largest wave. Note that the mean overtopping is given in l/s per m width and that the maximum overtopping volume is given in l per m width.

As example a smooth slope with slope angle 1:4 is taken, a rubble mound slope with a steeper slope of 1:1.5 and a vertical wall. The storm duration has been assumed as 2 hours (the peak of the tide) and a fixed wave steepness of $s_{om-1,0} = 0.04$ has been taken. Fig. 4.4 gives the $q - V_{max}$ lines for the three structures and for relatively small waves of $H_{m0} = 1$ m (red lines) and for fairly large waves of $H_{m0} = 2.5$ m (black lines).

A few conclusions can be drawn from Fig. 4.4. First of all, the ratio q/V_{max} is about 1000 for small q (roughly around 1 l/s per m) and about 100 for large q (roughly around 100 l/s per m). So, the maximum volume in the largest wave is about 100 – 1000 times larger than the mean overtopping discharge.

Secondly, the red lines are lower than the black lines, which means that for lower wave heights, *but similar mean discharge, q* , the maximum overtopping volume is also smaller. For example, a vertical structure with a mean discharge of 10 l/s per m gives a maximum volume

of 1000 l per m for a 1 m wave height and a volume of 4000 l per m for a 2.5 m wave height.

Finally, the three different structures give different relationships, depending on the equations to calculate q and the equations to calculate the number of overtopping waves. More information can be found in Chapters 5, 6 and 7.

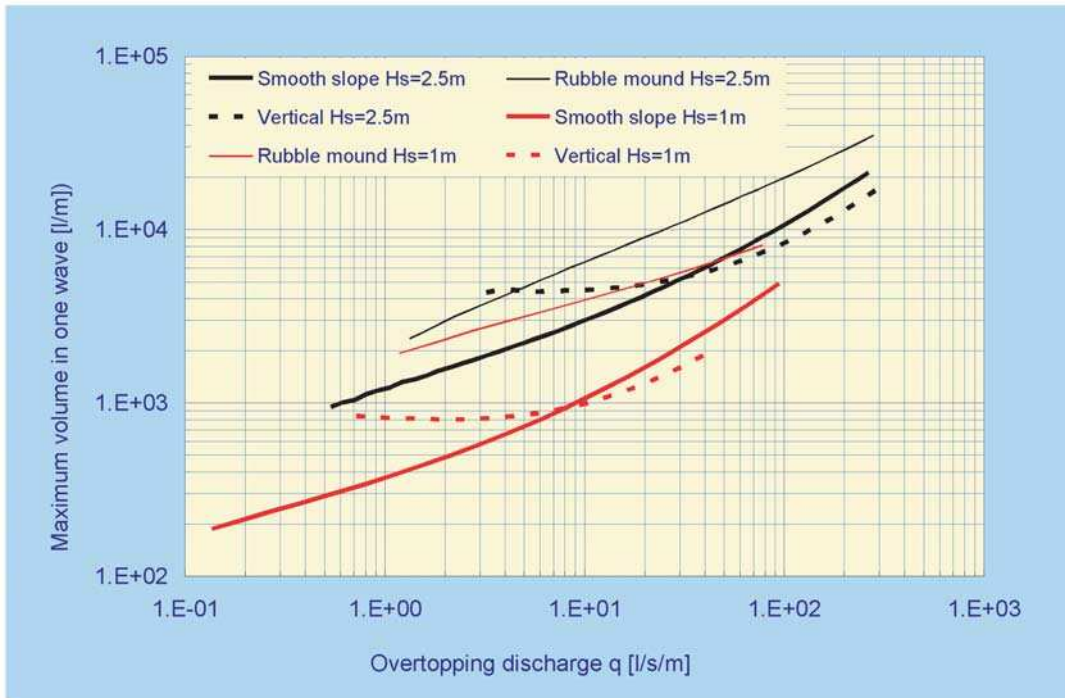


Fig. 4.4: Relationship between mean discharge and maximum overtopping volume in one wave for smooth, rubble mound and vertical structures for wave heights of 1 m and 2.5 m

4.2.3 Wave transmission by wave overtopping

Admissible overtopping depends on the consequences of this overtopping. If water is behind a structure, like for breakwaters and low-crested structures along the shore, large overtopping can be allowed as this overtopping will plunge into the water again. What happens is that the overtopping waves cause new waves behind the structure. This is called wave transmission and is defined by the wave transmission coefficient $K_t = H_{m0,t}/H_{m0,i}$, with $H_{m0,t}$ = transmitted significant wave height and $H_{m0,i}$ = incident significant wave height. The limits of wave transmission are $K_t = 0$ (no transmission) and 1 (no reduction in wave height). If a structure has its crest above water the transmission coefficient will never be larger than about 0.4–0.5.

Wave transmission has been investigated in the European DELOS project. For smooth sloping structures the following prediction formulae were derived:

$$K_t = \left[-0.3 \cdot \frac{R_C}{H_{m0,i}} + 0.75 \cdot (1 - \exp(-0.5 \cdot \xi_{0,p})) \right] \cdot (\cos \beta)^{2/3} \quad 4.5$$

with a minimum $K_t = 0.075$ and maximum $K_t = 0.8$, and limitations $1 < \xi_{op} < 3$, $0^\circ \leq \beta \leq 70^\circ$.

and $1 < B/H_i < 4$, and where β is the angle of wave attack and B is crest width (and not berm width).

Fig. 4.5 shows the transmission coefficient K_t as a function of the relative freeboard R_c/H_{m0} and for a smooth structure with slope angle $\cot\alpha = 4$ (a gentle smooth low-crested structure). Three wave steepnesses have been used: $s_{0,p} = 0.01$ (long waves), 0.03 and 0.05 (short wind waves). Also perpendicular wave attack has been assumed. Wave transmission decreases for increasing crest height and a longer wave gives more transmission. Wave overtopping can be calculated for the same structure and wave conditions, see Chapter 5 and Fig. 4.6. Also here a longer wave gives more wave overtopping.

The relationship between wave overtopping and transmission is found if both Fig.s are combined and Fig. 4.7 shows this relationship. For convenience the graphs are not made in a dimensionless way, but for a wave height of 3 m. A very small transmitted wave height of 0.1 m is only found if the wave overtopping is at least 30–50 l/s per m. In order to reach a transmitted wave height of about 1 m (one-third of the incident wave height) the wave overtopping should at least be 500–2500 l/s/m or 0.5–2.5 m³/s/m.

One may conclude that wave transmission is always associated with (very) large wave overtopping.

Wave transmission for rubble mound structures has also been investigated in the European DELOS project and the following prediction formulae were derived for wave transmission:

$$K_t = -0.4 R_c/H_{m0} + 0.64 B/H_{m0} - 0.31(1 - \exp(-0.5 \xi_{op})) \quad \text{for } 0.075 \leq K_t \leq 0.8 \quad 4.6$$

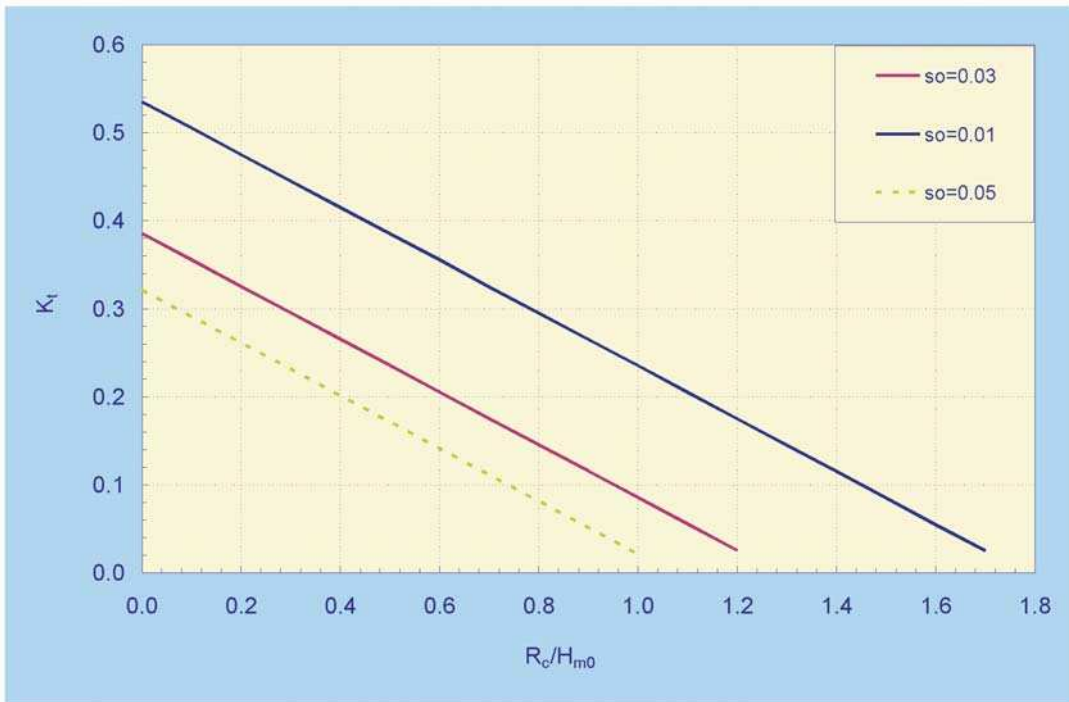


Fig. 4.5: Wave transmission for a gentle smooth structure of 1:4 and for different wave steepness

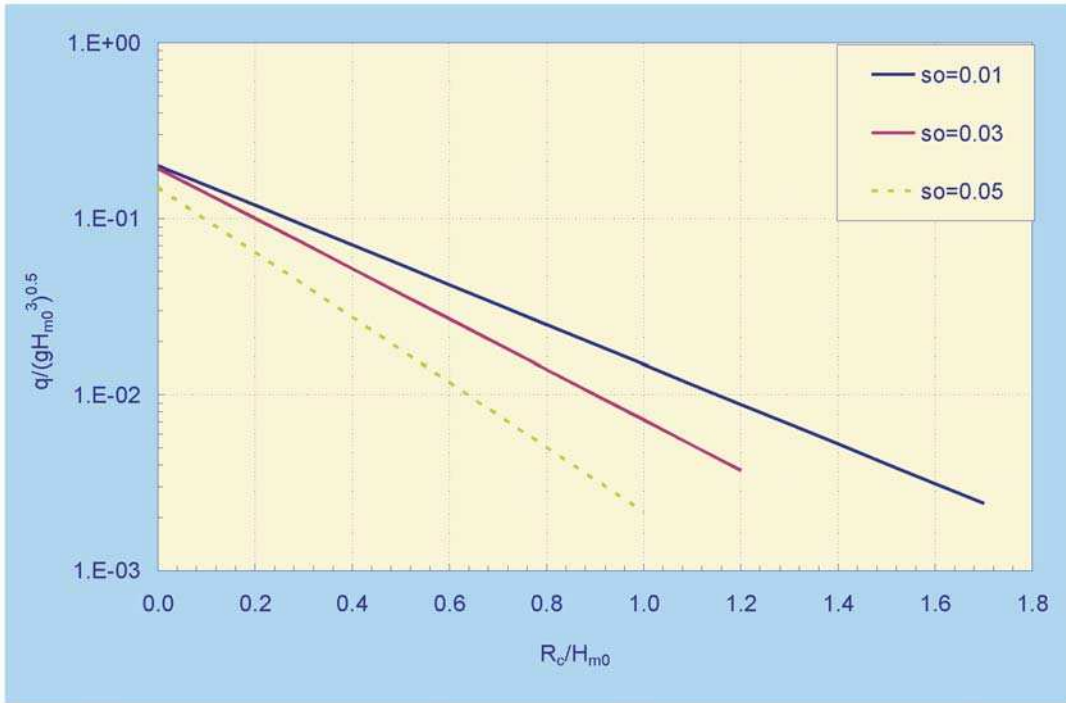


Fig. 4.6: Wave overtopping for a gentle smooth structure of 1:4 and for different wave steepness

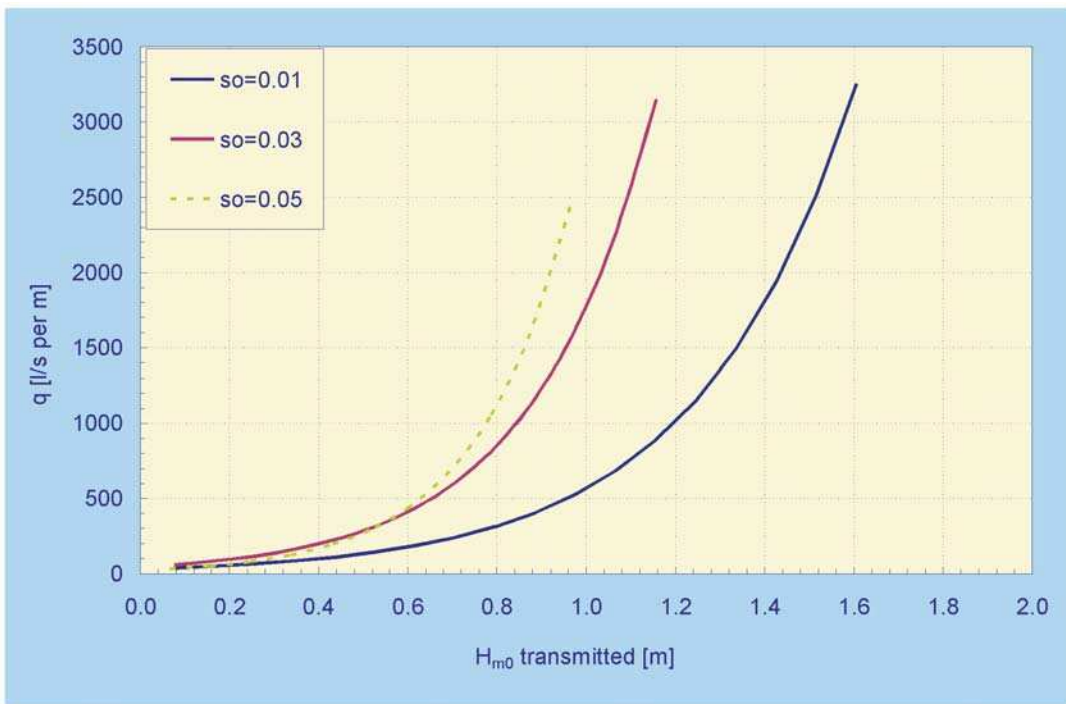


Fig. 4.7: Wave transmission versus wave overtopping for a smooth 1:4 slope and a wave height of $H_{m0} = 3$ m

Wave overtopping for a rubble mound structure with simple slope can be calculated by Equations in Chapter 6. A typical rubble mound structure has been used as example, with $\cot\alpha = 1.5$; 6–10 ton rock ($D_{n50} = 1.5$ m) as armour and a crest width of 4.5 m ($3 D_{n50}$). A wave height of 3 m has been assumed with the following wave steepness: $s_{0m-1,0} = 0.01$ (long waves), 0.03 and 0.05 (short wind waves). In the calculations the crest height has been changed to calculate wave transmission as well as wave overtopping.

Fig. 4.8 gives the comparison. The graph shows that a longer wave ($s_{0m1,0} = 0.01$) gives more wave transmission, for the same overtopping discharge. The reason could be that wave overtopping is defined at the rear of the crest, where (without superstructure or capping wall), waves can penetrate through the armour layer at the crest and generate waves behind the structure. This is easier for longer waves.

In contrast to smooth structures, one may conclude that even without considerable wave overtopping discharge at the rear of the crest, there still might be considerable wave transmission through the structure. In this example transmitted wave heights between 0.5 m and 1 m are found for overtopping discharges smaller than 100–200 l/s per m. Only larger transmitted wave heights are associated with extreme large overtopping discharges of more than 500–1000 l/s per m.

A simple equation for wave transmission at vertical structures has been given by GODA (2000):

$$K_t = 0.45 - 0.3 R_c/H_{m0} \quad \text{for } 0 < R_c/H_{m0} < 1.25 \quad 4.7$$

Wave overtopping for a simple vertical structure can be calculated by Equation 7.4. In both formulae only the relative crest height plays a role and no wave period, steepness or

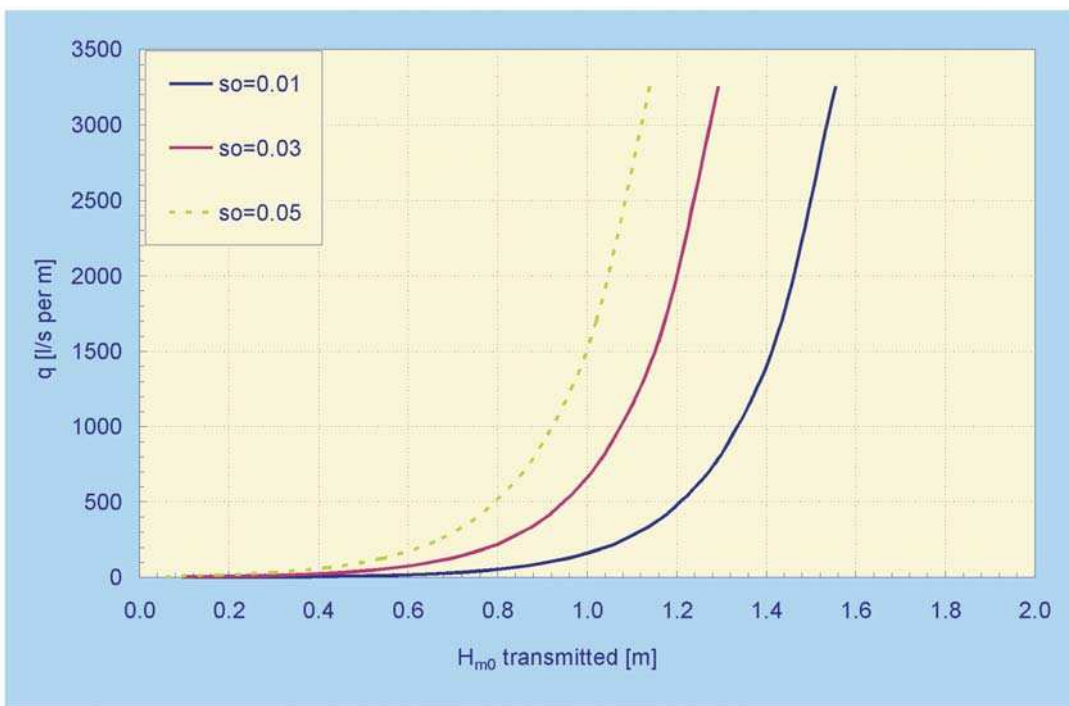


Fig. 4.8: Wave transmission versus wave overtopping discharge for a rubble mound structure, $\cot\alpha = 1.5$; 6–10 ton rock, $B = 4.5$ m and $H_{m0} = 3$ m

slope angle. A simple vertical structure has been used as example with a fixed incident wave height of $H_{m0} = 3$ m. Fig. 4.9 gives the comparison of wave overtopping and wave transmission, where in the calculations the crest height has been changed to calculate wave transmission as well as wave overtopping.

For comparison the same rubble mound structure has been used as the example in Fig. 4.8, with $\cot\alpha = 1.5$; 6–10 ton rock ($D_{n50} = 1.5$ m) as armour, a crest width of 4.5 m ($3 D_{n50}$) and a wave steepness $s_{op} = 0.03$. The curve for a smooth structure (Fig. 4.7) and for $s_{op} = 0.03$ has been given too in Fig. 7.24.

A rubble mound structure gives more wave transmission than a smooth structure, under the condition that the overtopping discharge is similar. But a vertical structure gives even more transmission. The reason may be that overtopping water over the crest of a vertical breakwater always falls from a distance into the water, where at a sloping structure water flows over and/or through the structure.

One may conclude that even without considerable wave overtopping discharge at the crest of a vertical structure, there still might be considerable wave transmission. In this example of a vertical structure, transmitted wave heights between 0.5 m and 1 m are found for overtopping discharges smaller than 100–200 l/s per m.

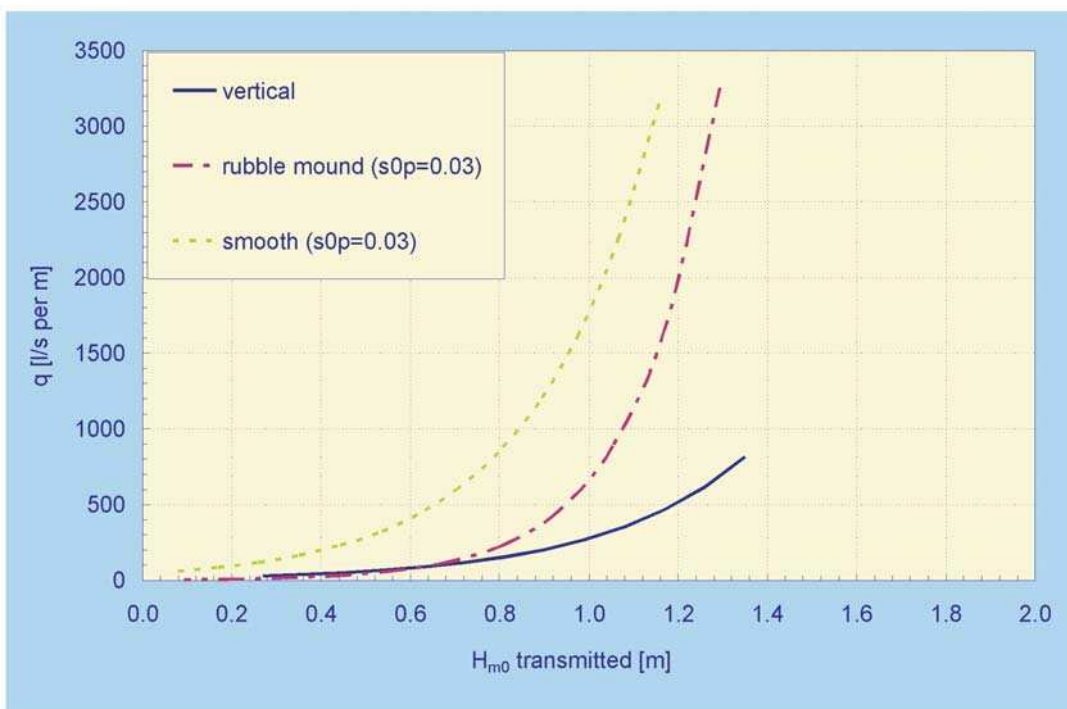


Fig. 4.9: Comparison of wave overtopping and transmission for a vertical, rubble mound and smooth structure



Fig. 4.10: Wave overtopping and transmission at breakwater IJmuiden, the Netherlands

4.3 P C - O v e r t o p p i n g

The programme PC-OVERTOPPING was made on the results of the Technical TAW Report “Wave run-up and wave overtopping at dikes” and is used for the 5-yearly safety assessment of all water defences in the Netherlands. The TAW Report has now in this Manual been replaced by Chapter 5 (dikes and embankments) and extended for rubble mound and vertical structures in Chapters 6 and 7. The programme was mainly based on a *dike type structure*. It means that the structure should be sloping, although a small vertical wall on top of the dike may be taken into account. Also roughness/permeability different from “smooth” can be taken into account, but not a crest with permeable and rough rock or armour units. In such a case the structure should be modelled up to the transition to the crest and other formulae should be used to take into account the effect of the crest (see Chapter 6).

The programme was set-up in such a way that almost *every sloping structure* can be modelled by an unlimited number of sections. Each section is given by x-y coordinates and each section can have its own roughness factor. The programme calculates almost all relevant overtopping parameters (except flow velocities and flow depths), such as:

- 2% run-up level;
 - mean overtopping discharge;
 - percentage of overtopping waves;
 - overtopping volumes per wave (maximum and for every percentage defined by the user);
 - required crest height for given mean overtopping discharges (defined by the user).
- The main advantages of PC-OVERTOPPING are:
- Modelling of each sloping structure, including different roughness along the slope;
 - Calculation of most overtopping parameters, not only the mean discharge.

The main disadvantage is:

- It does not calculate vertical structures and not a rough/permeable crest.

In order to show the capabilities of the programme an example will be given. Fig. 4.11 shows the cross-section of a dike with the design water level 1 m above CD. Different materials are used on the slope: rock, basalt, concrete asphalt, open concrete system and grass on the upper part of the structure. The structure has been schematised in Fig. 4.12 by x-y coordinates and a selection of the material of the top layer. The programme selects the right roughness factor.

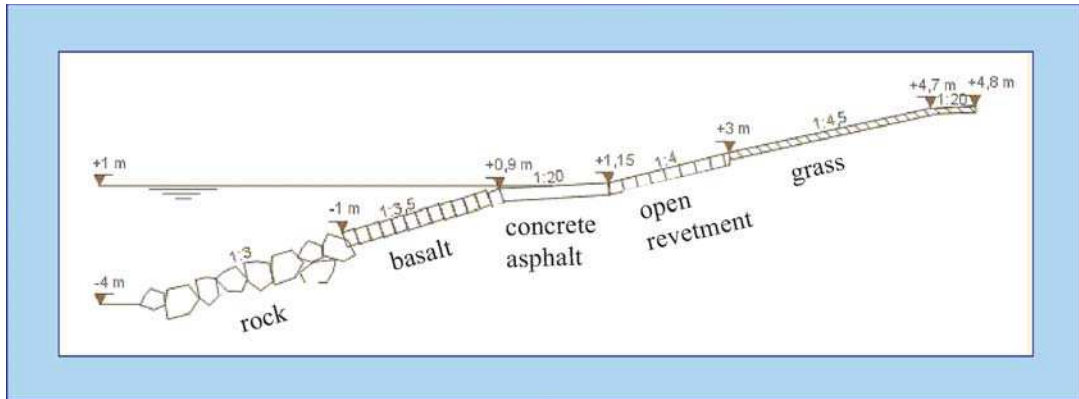


Fig. 4.11: Example cross-section of a dike

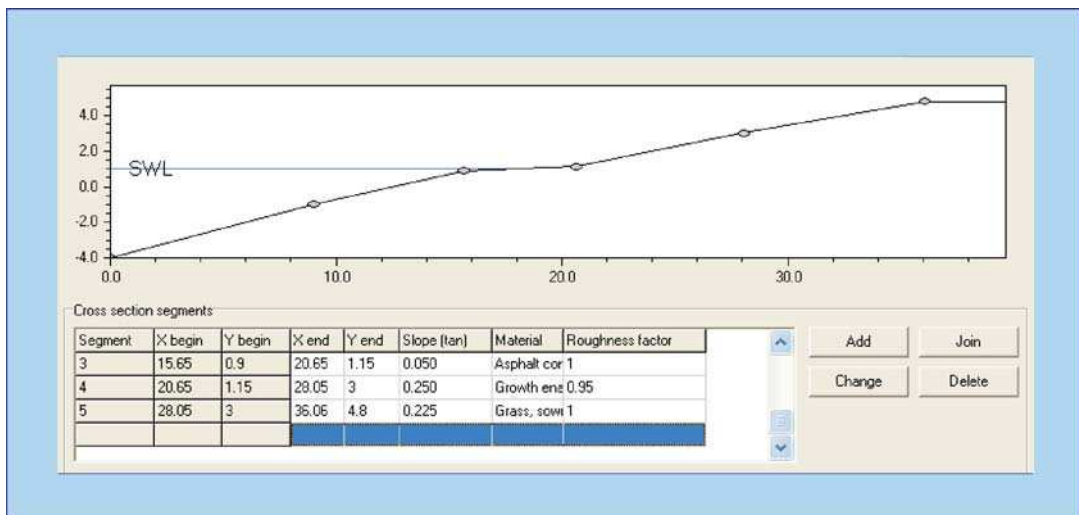


Fig. 4.12: Input of geometry by x-y coordinates and choice of top material

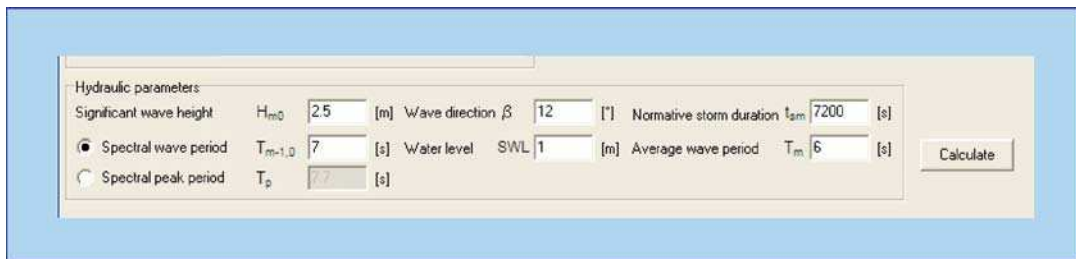


Fig. 4.13: Input file

The input parameters are the wave height, wave period (choice between the spectral parameter $T_{m-1,0}$ and the peak period T_p), the wave angle, water level (with respect to CD, the same level as used for the structure geometry) and finally the storm duration and mean period (for calculation of overtopping volumes, etc.). Fig. 4.13 gives the input file.

The output is given in three columns, see Fig. 4.14. The left column gives the 2% run-up level, the mean overtopping discharge and the percentage of overtopping waves. If the 2%-run-up level is higher than the actual dike crest, this level is calculated by extending the highest section in the cross-section. The middle column gives the required dike height for given mean overtopping discharges. Also here the highest section is extended, if required. Finally, in the right column the number of overtopping waves in the given storm duration are given, together with the maximum overtopping volume and other volumes, belonging to specified overtopping percentages (percentage of the number of overtopping waves).

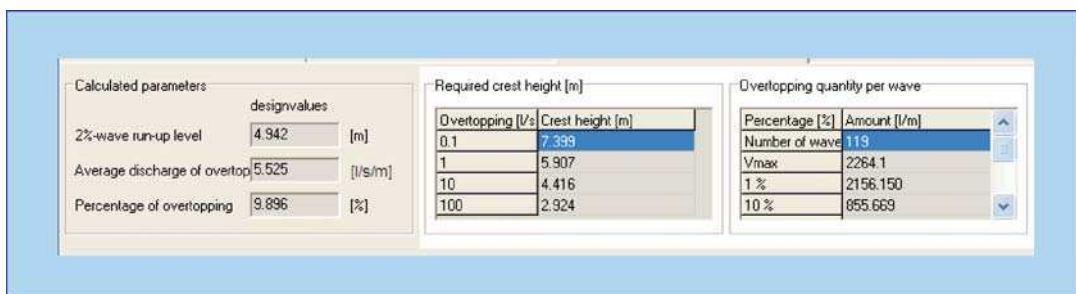


Fig. 4.14: Output of PC-OVERTOPPING

The programme also provides a kind of check whether found results of the 2% run-up level and mean overtopping discharge fall within measured ranges. All test results where the formulae were based on, are given in a run-up or overtopping graph, see Fig. 4.15 and Fig. 4.16. The graphs show the actual measured run-up or overtopping, including the effect of reductions due to roughness, berms, etc. The curve gives the maximum, which means a smooth straight slope with perpendicular wave attack. The programme then plots the calculated point in these graphs (the green point within the red circle).

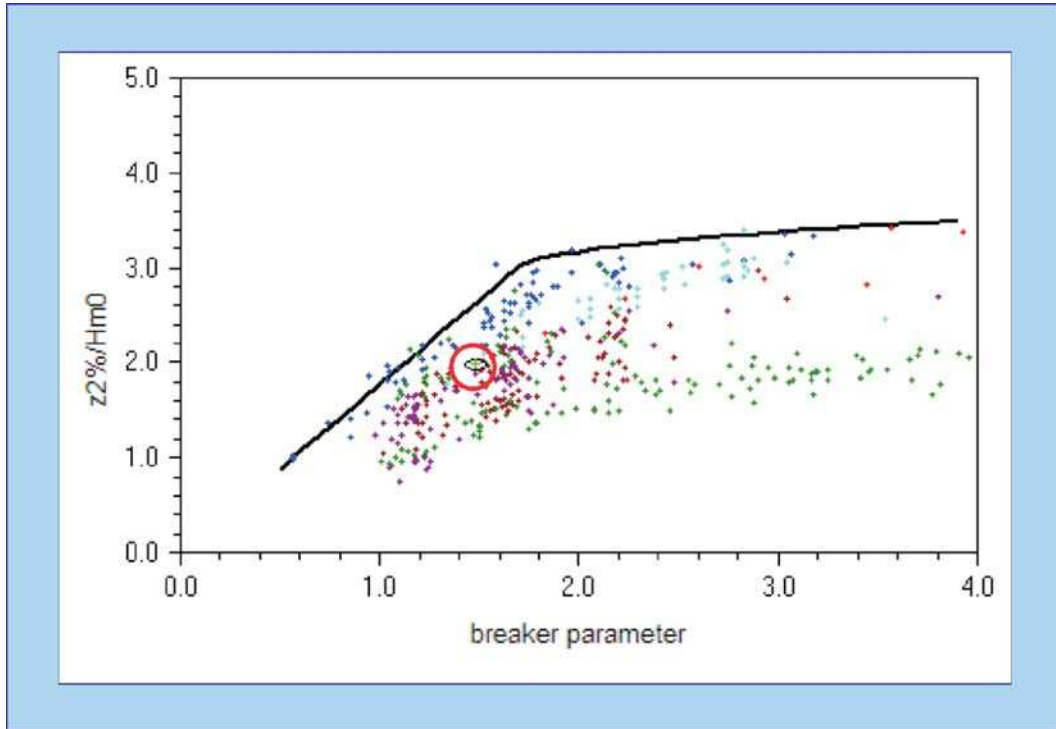


Fig. 4.15: Check on 2% run-up level

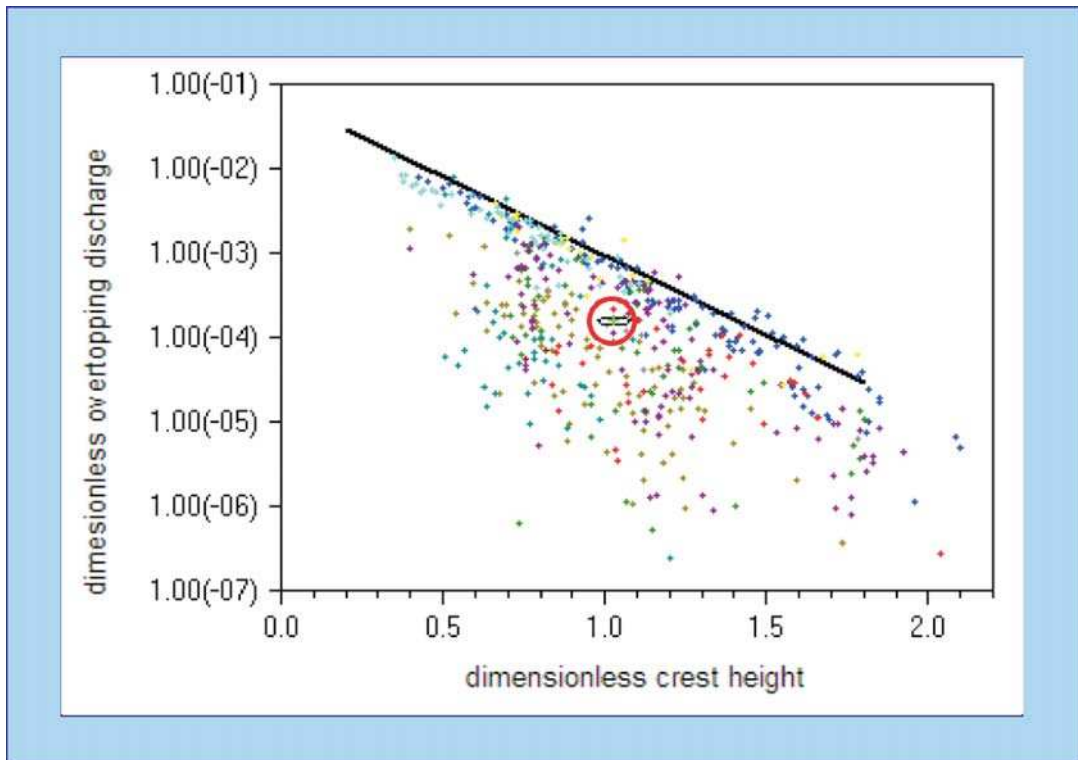


Fig. 4.16: Check on mean overtopping discharge

4.4 Neural network tools

Artificial neural networks fall in the field of artificial intelligence and can in this context be defined as systems that simulate intelligence by attempting to reproduce the structure of human brains. Neural networks are organised in the form of layers and within each layer there are one or more processing elements called 'neurons'. The first layer is the input layer and the number of neurons in this layer is equal to the number of input parameters. The last layer is the output layer and the number of neurons in this layer is equal to the number of output parameters to be predicted. The layers in between the input and output layers are the hidden layers and consist of a number of neurons to be defined in the configuration of the NN. Each neuron in each layer receives information from the preceding layer through the connections, carries out some standard operations and produces an output. Each connectivity has a weight factor assigned, as a result of the calibration of the neural network. The input of a neuron consists of a weighted sum of the outputs of the preceding layer; the output of a neuron is generated using a linear activation function. This procedure is followed for each neuron; the output neuron generates the final prediction of the neural network.

Artificial neural networks have applications in many fields and also in the field of coastal engineering for prediction of rock stability, forces on walls, wave transmission and wave overtopping. The development of an artificial neural network is useful if:

- the process to be described is complicated with a lot of parameters involved,
- there is a large amount of data.

Less complicated processes may be described by empirical formulae. This is also true for the process of wave overtopping, where many formulae exist, but always for a certain type of structure. Wave overtopping on all kind of structures can not be covered by only one formula, but a neural network is able to do this. A neural network needs a large amount of data to become useful for prediction. If the amount of data is too small, many predictions might be unreliable as the prediction will be out of range. But specially for the topic of wave overtopping there is an overwhelming amount of tests on all kinds of coastal structures and embankments.

This was the reason to start the European CLASH project. The result has been that two neural networks have been developed, one within CLASH and one along side of CLASH as a PhD-work. In both cases the neural network configuration was based on Fig. 4.17, where the input layer has 15 input parameters ($\beta, h, H_{m0toe}, T_{m-1,0toe}, h_t, B_t, \gamma_\beta, cot\alpha_d, cot\alpha_w, R_c, B, h_b, tan\alpha_b, A_c, G_c$) and 1 output parameter in the output layer (i.e. mean overtopping discharge, q). CLASH was focused on a three-layered neural network, where a configuration with one single hidden layer was chosen.

The development of an artificial neural network is a difficult task. All data should be checked thoroughly (rubbish in = rubbish out) and the training of a neural network needs special skills. The application of a developed neural network as a prediction tool, however, is easy and can be done by most practical engineers! It is for this reason that the CLASH neural network is part of this manual.

The application of the neural network is providing an Excel or ASCII input file with parameters, run the programme (push a button) and get a result file with mean overtopping discharge(s). Such an application is as easy as getting an answer from a formula programmed in Excel and does not need knowledge about neural networks. The advantages of the neural network are:

- it works for almost every structure configuration,
- it is easy to calculate trends instead of just one calculation with one answer.

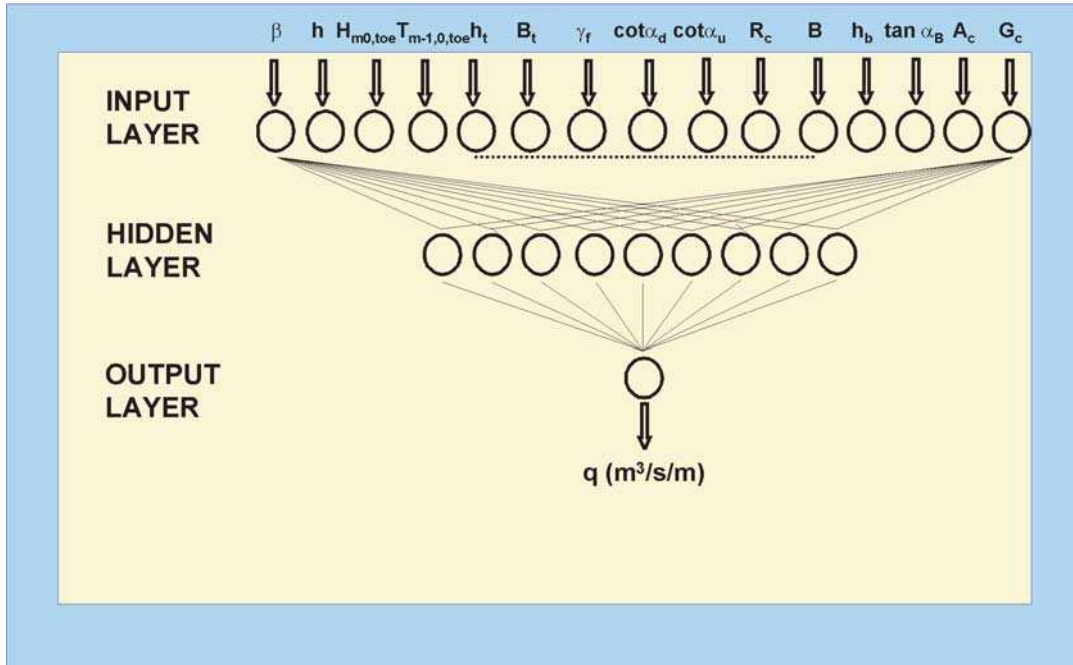


Fig. 4.17: Configuration of the neural network for wave overtopping

The input exists of 10 structural parameters and 4 hydraulic parameters. The hydraulic parameters are wave height, wave period, and wave angle and water depth just in front of the structure. The structural parameters describe almost every possible structure configuration by a toe (2 parameters), two structure slopes (including vertical and wave return walls), a berm (2 parameters) and a crest configuration (3 parameters). The tenth structural parameter is the roughness factor for the structure (γ_f) and describes the *average roughness of the whole structure*. Although guidance is given, estimation is not easy if the structure has different roughness on various parts of the structure. An overall view of possible structure configurations is shown in Fig. 4.18. It clearly shows that the neural network is able to cope with most structure types.

Very often one is not only interested in one calculation, but in more. As the input file has no limitations in number of rows (= number of calculations), it is easy to incrementally increase one or more parameters and to find a trend for a certain (design) measure. As example for calculation of a trend with the neural network tool an example cross-section of a rubble mound embankment with a wave wall has been chosen, see Fig. 4.19.

If, for example, the cross-section in Fig. 4.19 would have too much overtopping, the following measures could be considered:

- Increasing the crest
- Applying a berm
- Widening the crest
- Increasing only the crest wall.

Table 4.1 shows the input file with the first 6 calculations, where incremental increase of the crest will show the effect of raising the crest on the amount of wave overtopping. Calculations will give an output file with the mean overtopping discharge q (m^3/s per m width) and

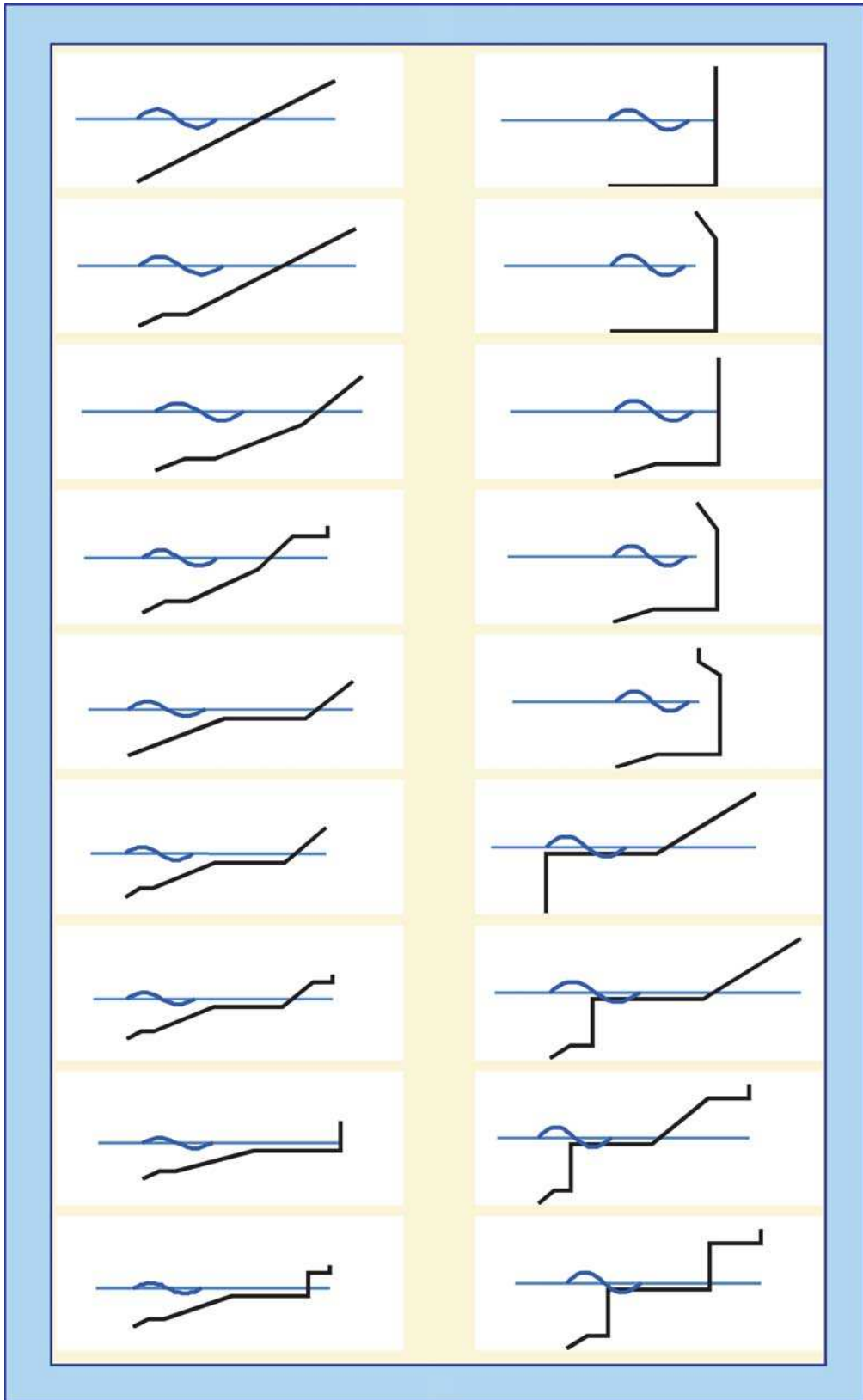


Fig. 4.18: Overall view of possible structure configurations for the neural network

with confidence limits. Table 4.2 shows an example which is the output belonging to the input in Table 4.1.

Table 4.1: Example input file for neural network with first 6 calculations

β	h	H_{m0}	$T_{m-1,0}$	h_t	B_t	γ_r	$\cot\alpha_d$	$\cot\alpha_u$	R_c	B	h_b	$\tan\alpha_B$	A_c	G_c
0	12	5	9.1	9	4	0.49	1.5	1.5	4	0	0	0	5	5
0	12	5	9.1	9	4	0.49	1.5	1.5	4.05	0	0	0	5.05	5
0	12	5	9.1	9	4	0.49	1.5	1.5	4.1	0	0	0	5.1	5
0	12	5	9.1	9	4	0.49	1.5	1.5	4.15	0	0	0	5.15	5
0	12	5	9.1	9	4	0.49	1.5	1.5	4.2	0	0	0	5.2	5
0	12	5	9.1	9	4	0.49	1.5	1.5	4.25	0	0	0	5.25	5

Table 4.2: Output file of neural network with confidence limits

q (m ³ /s/m)	2.50%	5.00%	25.00%	50.00%	75.00%	95.00%	97.50%	Nr.Pat.	REMARK I
5.90E-02	2.45E-02	2.77E-02	4.15E-02	5.91E-02	8.35E-02	0.1299	0.1591	1	4
5.64E-02	2.35E-02	2.64E-02	3.99E-02	5.58E-02	7.91E-02	0.1246	0.1516	2	4
5.40E-02	2.26E-02	2.49E-02	3.82E-02	5.33E-02	7.52E-02	0.119	0.1448	3	4
5.16E-02	2.19E-02	2.39E-02	3.69E-02	5.08E-02	7.17E-02	0.1133	0.1383	4	4
4.94E-02	2.07E-02	2.27E-02	3.55E-02	4.85E-02	6.89E-02	0.1079	0.1324	5	4
4.73E-02	1.99E-02	2.18E-02	3.38E-02	4.62E-02	6.60E-02	0.1033	0.1265	6	4

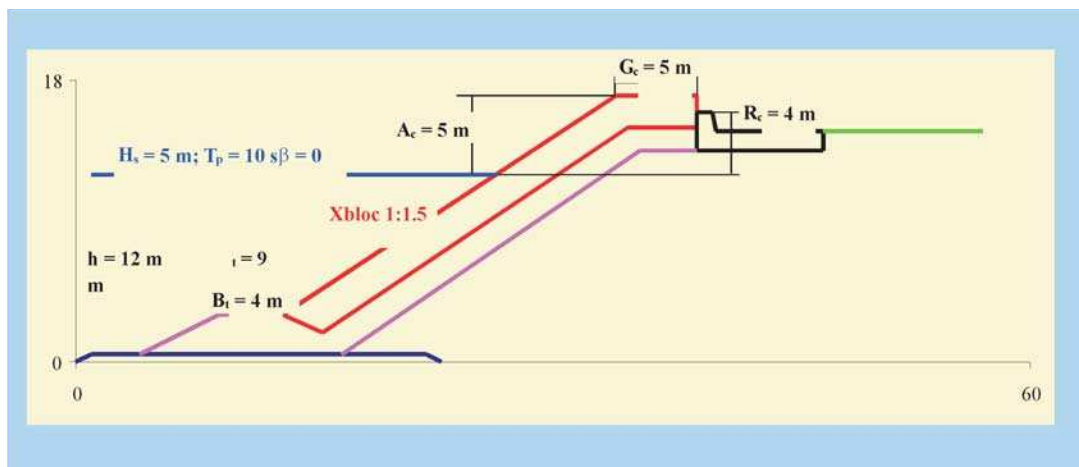


Fig. 4.19: Example cross-section with parameters for application of neural network

To make the input file for this example took 1 hour and resulted in 1400 rows or calculations. The calculation of the neural network took less than 10 seconds. The results were copied into the Excel input file and a resulting graph was made within Excel, which took another hour. Fig. 4.20 gives the final result, where the four trends are shown. The base situation had an overtopping discharge of 59 l/s per m. The graph clearly shows what measures are required to reduce the overtopping by for example a factor 10 (to 5.9 l/s per m) or to only 1 l/s per m. It also shows that increasing structure height is most effective, followed by increasing only the crest wall.

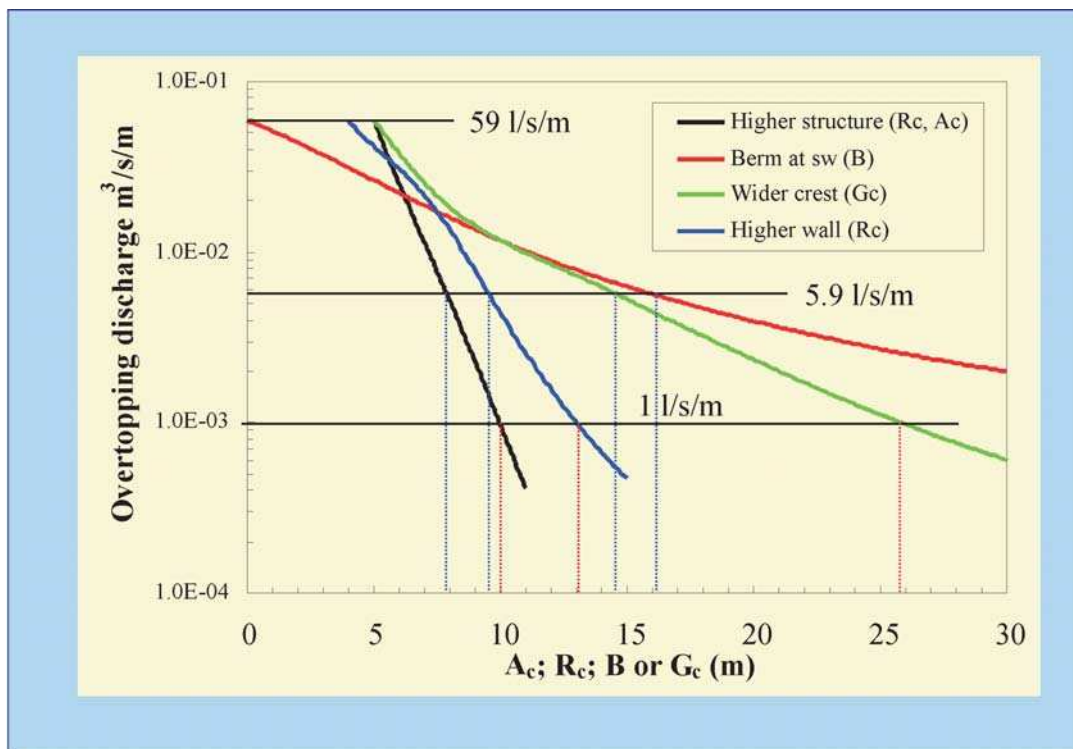


Fig. 4.20: Results of a trend calculation

At present two neural networks exist. One is the official neural network developed by Delft Hydraulics in the CLASH project. It runs as an executable and can be downloaded from the CLASH website or the Manual website. The other neural network has also been developed within CLASH, but as part of a PhD-thesis at Gent University (VERHAEGHE, 2005). The network was developed in MatLab® and actually an application can only be performed if the user has MatLab®, which is not often the case in the engineering world. An easier application has to be worked out: web based or executable.

The advantage of the Gent neural network is that it first decides whether there will be overtopping or not (classifier). If there is no overtopping it will give $q = 0$. If there is overtopping, it will quantify the overtopping with a similar network as the CLASH network (quantifier). This is certainly an advantage above the CLASH network. The CLASH network was only trained with overtopping data (tests with “no overtopping” were not considered) and, therefore, this network always gives a prediction of overtopping, also in the range where no overtopping should be expected.

4.5 Use of CLASH database

The EU-programme CLASH resulted in an extensive database with wave overtopping tests. Each test was described by 31 parameters as hydraulic and structural parameters, but also parameters describing the reliability and complexity of the test and structure. The database includes more than 10,000 tests and was set-up as an Excel database. The database, therefore, is nothing more than a matrix with 31 columns and more than 10,000 rows.

If a user has a specific structure, there is a possibility to look into the database and find more or less similar structures with measured overtopping discharges. It may even be possible that the structure has already been tested with the right wave conditions! Finding the right tests can be done by using filters in the Excel database. Every test of such a selection can then be studied thoroughly. One example will be described here in depth.

Suppose one is interested in improvement of a *vertical wall with a large wave return wall*. The wave conditions are $H_{m0\text{toe}} = 3$ m, the wave steepness $s_o = 0.04$ ($T_{m-1,0} = 6.9$ s) and the wave attack is perpendicular to the structure. The design water depth $h = 10$ m and the wave return wall starts 1 m above design water level and has a height and width of 2 m (the angle is 45° seaward). This gives a crest freeboard $R_c = 3$ m, equal to the wave height. Have tests been performed which are close to this specific structure and given wave conditions?

The first filter selects data with a vertical down slope, i.e. $\cot\alpha_u = 0$. The second filter could select data with a wave return wall overhanging more than about 30° seaward. This means $\cot\alpha_u < -0.57$. In first instance every large wave return wall can be considered, say at least $0.5 H_{m0}$ wide. This gives the third filter, selecting data with $-\cot\alpha_u * (A_c + h_b)/H_{m0} \geq 0.5$. With these 3 filters, the database gives 212 tests from 4 independent test series.

Fig. 4.21 shows the data together with the expression of FRANCO et al. (1994) for a vertical wall. There are 22 tests without overtopping. They are represented in the Fig. with a value of $q/(gH_{m0\text{toe}}^3)^{1/2} = 10^{-7}$. The majority of the data is situated below the curve for a vertical wall, indicating that a wave return wall is efficient, but the data is too much scattered to be decisive.

A next step in the filtering process could be that only wave return walls overhanging more than 45° seaward are selected. This means $\cot\alpha_u < -1$. The water depth is relatively large for the considered case and shallow water conditions are excluded if $h/H_{m0\text{toe}} > 3$. Fig. 4.22 shows this further filtering process. The number of data has been reduced to 78 tests from only 2 independent series. In total 12 tests result in no overtopping. The data show the trend that the overtopping is in average about ten times smaller than for a vertical wall, given by the dashed line. But for $R_c/H_{m0\text{toe}} > 1$ there are quite some tests without any overtopping.

As still quite some data are remaining in Fig. 4.22, it is possible to narrow the search area even further. With a wave steepness of $s_o = 0.04$ in the considered case, the wave steepness range can be limited to $0.03 < s_o < 0.05$. The width of the wave return wall of 2 m gives with the wave height of 3 m a relative width of 0.67. The range can be limited to $0.5 < -\cot\alpha_u * (A_c + h_b)/H_{m0} < 0.75$. Finally, the transition from vertical to wave return wall is 1 m above design water level, giving $h_b/H_{m0\text{toe}} = -0.33$. The range can be set at $-0.5 < h_b/H_{m0\text{toe}} < -0.2$.

The final selection obtained after filtering is given in Fig. 4.23. Only 4 tests remain from one test series, one test resulted in no overtopping. The data give now a clear picture. For a relative freeboard lower than about $R_c/H_{m0\text{toe}} = 0.7$ the overtopping will not be much different from the overtopping at a vertical wall. The wave return wall, however, becomes very efficient for large freeboards and even gives no overtopping for $R_c/H_{m0\text{toe}} > 1.2$. For the structure considered with $R_c/H_{m0\text{toe}} = 1$ the wave overtopping will be 20–40 times less than for a vertical wall and will probably amount to $q = 0.5\text{--}2$ l/s per m width. In this particular

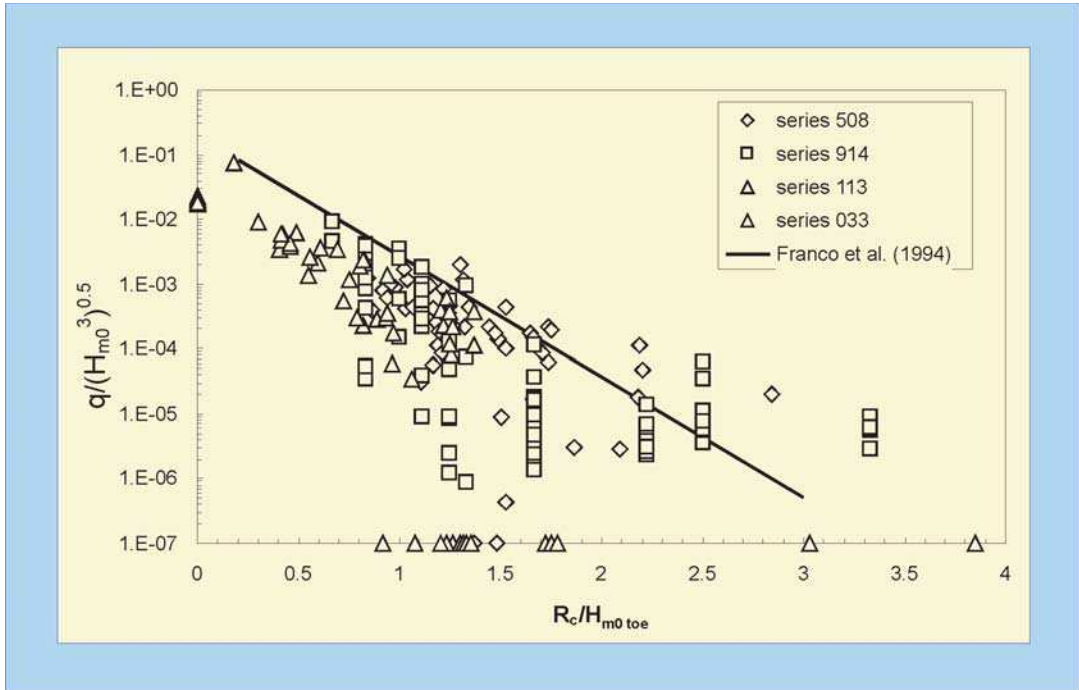


Fig. 4.21: Overtopping for large wave return walls; first selection

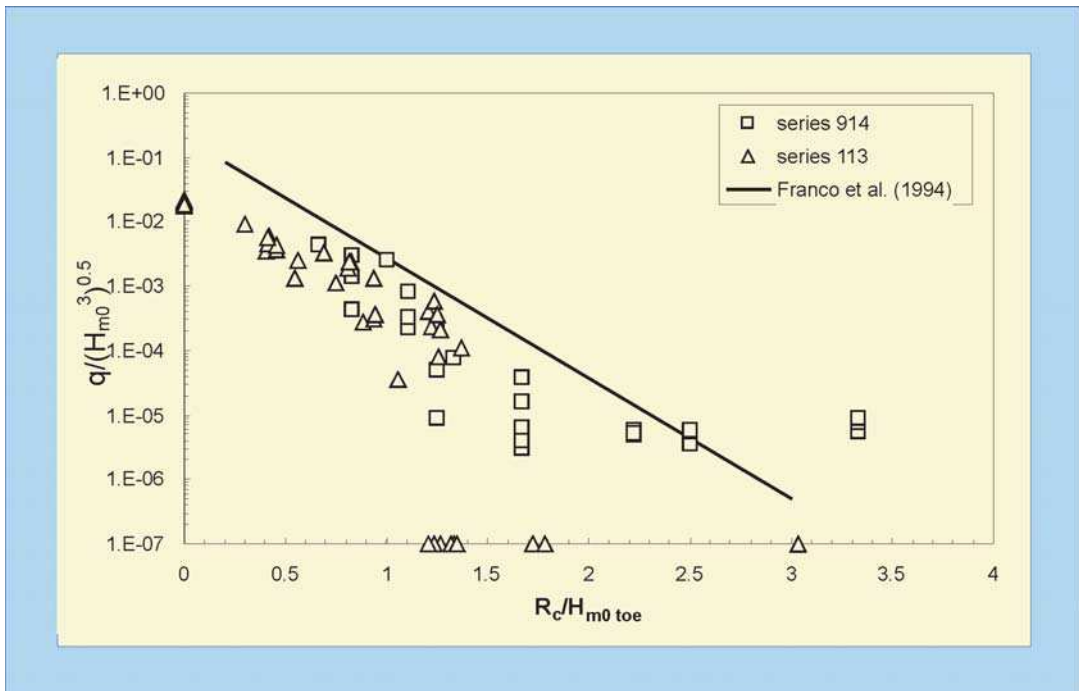


Fig. 4.22: Overtopping for large wave return walls; second selection with more criteria

case it was possible to find 4 tests in the database with very close similarities to the considered structure and wave conditions.

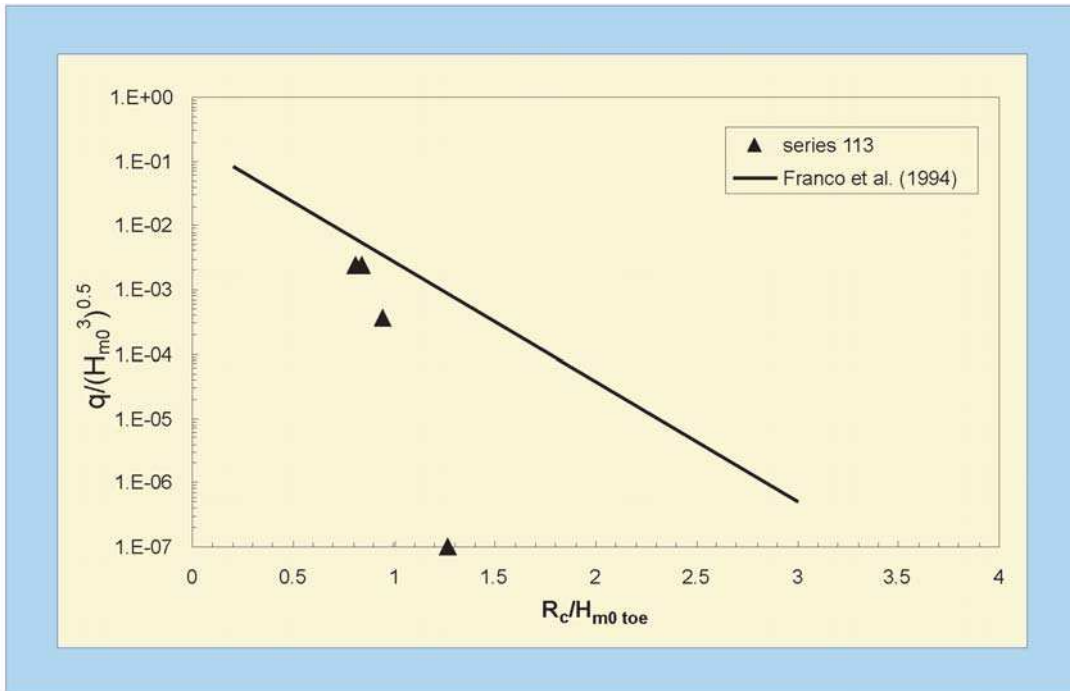


Fig. 4.23: Overtopping for a wave return wall with $s_o = 0.04$, seaward angle of 45° , a width of 2 m and a crest height of $R_c = 3$ m. For $H_{m0\ toe} = 3$ m the overtopping can be estimated from $R_c/H_{m0\ toe} = 1$

4.6 Outline of numerical model types

Empirical models or formulae use relatively simple equations to describe wave overtopping discharges in relation to defined wave and structure parameters. Empirical equations and coefficients are, however, limited to a relatively small number of simplified structure configurations. Their use out of range, or for other structure types, may require extrapolation, or may indeed not be valid. Numerical models of wave overtopping are less restrictive, in that any validated numerical model can; in theory; be configured for any structure within the overall range covered.

Realistic simulations of wave overtopping require numerical methods which are able to simulate shoaling, breaking on or over the structure, and possible overturning of waves. If there is violent or substantial wave breaking, or impulsive of waves onto the structure, then the simulations must be able to continue beyond this point. Wave attack on permeable coastal structures with a high permeability, such as those consisting of coarse granular material or large artificial blocks, cannot be modelled without modelling the porous media flow. The energy dissipation inside the permeable parts, the infiltration and seepage in the swash and backwash area, and the interactive flow between the external wave motion and the internal wave motion often cause the wave attack to be quite different from the flow on impermeable structures.

All of the processes described above occur during overtopping at structures, and all affect how the wave overtops and determine the peak and mean discharges. Additionally, physical model tests suggest that a sea state represented by 1000 random waves will give reasonably consistent results, but that shorter tests may show significant variations in extreme statistics. Any numerical model should therefore be capable of running similar numbers of waves.

There are no numerical models capable of meeting all of the above criteria accurately in a computationally effective or economical way, and it may be many more years before advances in computer technology allow these types of models to be used. There are, however, different model types each capable of meeting some of these criteria. They essentially fall into two principal categories: the nonlinear shallow water equation models (NLSW); and those based on the Navier-Stokes equations. Each of these generic types will now be discussed, with the emphasis on the range of applicability rather than the underlying mathematical principals.

4.6.1 Navier-Stokes models

The fluid motion for models based on the Navier-Stokes equations will generally be controlled by one of two principal techniques: the Volume of Fluid (VOF) method first described by HIRT & NICHOLS (1981); and the Smooth Particle Hydrodynamics (SPH) method as discussed by MONAGHAN (1994). Each of these models requires a detailed computational grid to be defined throughout the fluid domain, with solutions to the complex set of equations required at each grid-point before the simulation can continue. Restricted to only two dimensions, and for computational domains of only two or three wavelengths, these model types will typically take several minutes of computational time to simulate small fractions of a second of real time. In general SPH models take longer to run than VOF models.

An example of a model based on the Navier-Stokes equations is the VOF model SKYLLA. Developed to provide a wide range of applicability, high accuracy and a detailed description of the flow field for a wide range of structures, including permeable structures. It includes combined modelling of free surface wave motion, and porous media flow, and allows for simulations with large variations in the vertical direction in both the flow field and in the cross section of the structure. The internal wave motion is simulated within the porous media flow, and is valid for 2d incompressible flow with constant fluid mass density through a homogeneous isotropic porous medium. It is, nevertheless, restricted to regular waves, since irregular waves cannot be computed within manageable computational times.

Although computationally very expensive, these model types can provide descriptions of pressure and velocity fields within porous structures, and impulsive and breaking wave loads. Computation of wave transmission and wave run-up of monochromatic waves is possible, but the study of more than a few irregular overtopping waves is not yet possible.

4.6.2 Nonlinear shallow water equation models

The one-dimensional shallow water equations were originally developed for near horizontal, free-surface channel flows. The equations describe water depth and horizontal velocity in time and space, where vertical velocity is neglected, and only hydrostatic pressure is considered. The resulting nonlinear shallow water (NLSW) equations; derived from the

Navier-Stokes equations; simplify the mathematical problem considerably, allowing realistic, but simplified, real-time simulations to be computed.

The general restriction of these models is that they must be in shallow water ($h/L < 0.05$) if the model assumptions are to be preserved, and that waves entering into the computational domain have or will break. The fundamental mathematical assumption for NLSW models is that the waves travel as bores as described by HIBBERD & PEREGRINE (1979). At the crest of a sea defence structure, these models are able to continue computing as the flows either side of the crest separate, overtop or return.

ODIFLOCS (VAN GENT, 1994) is a one-dimensional, time-domain model which simulates the wave attack of perpendicular incident waves on permeable and impermeable coastal structures. The NLSW model is coupled to an internal porous media flow model (KOBAYASHI et al., 1987) that allows homogenous permeable structures to be modelled. This allows the modelling of infiltration and seepage phenomena, and the internal phreatic surface can be followed separately from the free surface flow. ODIFLOCS was developed to estimate permeability coefficients, wave transmission, magnitude of internal set-up, and the influence of spectral shape on wave run-up and overtopping.

The ANEMONE model suite developed by DODD (1998), comes as both a 1d and a 2d plan model, and also incorporates a porous media flow model for examining beaches (CLARKE et al., 2004). The landward boundaries, both for the free surface flow and for the internal boundary of the porous media flow, can be modelled as open or closed (non-reflecting or fully reflecting respectively). The model is capable of simulating storms of a 1000 waves or more at little computational cost, recording wave-by-wave and mean overtopping discharges.

These models, and others like them, are invaluable tools to examine the difference in overtopping performance when modifications to a scheme design are to be investigated. Long wave runs for a variety of sea states, for say a range of crest levels, is a problem well suited to these models. The overtopping discharges computed by these models should not, however, be relied upon as this is generally a function of how the model is set up for a given study: e.g. specification of the position of the seaward boundary in the model will affect the overtopping rate. The absolute difference in overtopping between two similar runs will usually produce reliable information.

4.7 Physical modelling

Physical model tests are an established and reliable method for determining mean wave overtopping discharges for arbitrary coastal structural geometries; additional levels of sophistication allow individual overtopping volumes to be measured. Typically at Froudian scales of 1:5 to 1:50, models represent the prototype structure in 2d or 3d, and frequently occurring and extreme storm events can be modelled. Wave flumes are usually of 0.3 to 1.5 m width with a depth of 0.5 to 1.0 m and fitted with a piston based wave paddle. Some form of wave absorbing system to compensate for waves reflected from the model structure is essential for overtopping studies in wave flumes. Wave basin models vary in size and complexity, and overtopping may often be measured at several locations on the model.

Physical model tests are particularly useful when assessing wave overtopping, as overtopping is affected by several factors whose individual and combined influences are still largely unknown and difficult to predict. The most common hydraulic parameters which influence wave overtopping are the significant wave height, the wave period, the wave direc-

tion (obliquity), and the water depth at the structure toe. The structural parameters are the slope, the berm width and level, the crest width and level, and the geometry of any crest/parapet wall. Where rock or concrete armour are used the porosity, permeability and placement pattern of armour units affect overtopping as does the roughness of the individual structural elements.

Due to the large number of relevant parameters, and the very complex fluid motion at the structure, theoretical approaches to wave overtopping are not well developed. Physical model tests, such as wave flume studies, are therefore commonly used to develop empirical formulae for predicting wave overtopping. These formulae do not assess wave overtopping discharges and individual volumes accurately, especially for low overtopping volumes, rather they provide an order of magnitude approximation. This is partially caused by so far unknown scale and model effects and the fact that only very limited field data exists. These scale and model effects are briefly discussed in the following section.

There are many cases where there are no reliable empirical overtopping prediction methods for a given structure geometry, or where the performance of a particular scheme to reduce overtopping is especially sensitive: e.g. where public safety is a concern. Alternatively, it may be that the consequences of overtopping are important: e.g. where overtopping waves cause secondary waves to be generated in the lee of the structure. For cases such as these, physical model testing may be the only reliable option for assessing overtopping.

4.8 Model and Scale effects

This section deals with model and scale effects resulting from scaled hydraulic models on wave overtopping. First, definitions will be given what scale effects and model effects are. Secondly, a methodology based on the current knowledge is introduced on how to account for these effects.

4.8.1 Scale effects

Scale effects result from incorrect reproduction of a prototype water-structure interaction in the scale model. Reliable results can only be expected by fulfilling Froude's and Reynolds' law simultaneously. This is however not possible so that scale effects cannot be avoided when performing scaled model tests.

Since gravity, pressure and inertial forces are the relevant forces for wave motion most models are scaled according to Froude's law. Viscosity forces are governed by Reynolds' law, elasticity by Cauchy's law and surface tension forces by Weber's law, and these forces have to be neglected for most models. All effects and errors resulting from ignoring these forces are called scale effects. The problem of the quantification of these scale effects is still unresolved.

4.8.2 Model and measurement effects

Model or laboratory effects originate from the incorrect reproduction of the prototype structure, geometry and waves and currents, or due to the boundary conditions of a wave flume (side walls, wave paddle, etc.). Modelling techniques have developed significantly, but there are still influences of model effects on hydraulic model results to be expected.

Measurement effects result from different measurement equipment used for sampling the data in the prototype and model situations. These effects, which are referred to as “measurement effects” may significantly influence the comparison of results between prototype and model, or two identical models. It is therefore essential to quantify the effects and the uncertainty related to the different techniques available.

4.8.3 Methodology

Following the aforementioned definitions the reasons for differences in between model and prototype data will sometimes be very difficult to assign to either model or scale effects. During CLASH, the major contributions to model effects were found to be wind since this is ignored in the hydraulic model. Despite the lack of wind, additional differences were found and assigned to be due to model effects. The following phenomena may give indications of the contributions of the most important model effects in addition to wind. The repeatability of tests showed that the wave parameters (H_{m0} , T_p , $T_{m-1,0}$) have a coefficient of variation of $CoV \sim 3\%$, and for wave overtopping the differences between two wave flumes were $CoV \sim 13\%$ and $CoV \sim 10\%$. Different time windows for wave analysis and different types of wave generation methods had no influence on the estimated wave parameters ($CoV \sim 3\%$). The number of waves in the flume shows influence on wave overtopping, where a comparison of 200 compared to 1000 generated waves show differences in mean overtopping rates up to a value of 20%. The position of the overtopping tray at the side of the flume showed also differences in overtopping rates ($CoV \sim 20\%$) from results where the tray was located at the centre of the crest. This could be because of the different arrangement of the armour units in front of the overtopping tray or due to the influence of the side walls of the flume. More details on measurements and model effects are provided by KORTENHAUS et al. (2004a).

Scale effects have been investigated by various authors, and this has led to some generic rules that should be observed for physical model studies. Generally, water depths in the model should be much larger than $h = 2.0$ cm, wave periods larger than $T = 0.35$ s and wave heights larger than $H_s = 5.0$ cm to avoid the effects of surface tension; for rubble mound breakwaters the Reynolds number for the stability of the armour layer should exceed $Re = 3 \times 10^4$; for overtopping of coastal dikes $Re > 1 \times 10^3$; and the stone size in the core of rubble mound breakwaters has to be scaled according to the velocities in the core rather than the stone dimensions, especially for small models. The method for how this can be achieved is given in BURCHARTH et al. (1999). Furthermore, critical limits for the influence of viscosity and surface tension are given in Table 4.3, more details can be found in SCHÜTTRUMPF and OUMERACI (2005).

Table 4.3: Scale effects and critical limits

Process	Relevant forces	Similitude law	Critical limits
Wave propagation	Gravity force Friction forces Surface tension	Fr_W Re_W We	$Re_W > Re_{W,crit} = 1 \times 10^4$ $T > 0,35 \text{ s}; h > 2,0 \text{ cm}$
Wave breaking	Gravity force Friction forces Surface tension	Fr_W Re_W We	$Re_W > Re_{W,crit} = 1 \times 10^4$ $T > 0,35 \text{ s}; h > 2,0 \text{ cm}$
Wave run-up	Gravity force Friction forces Surface tension	Fr_A, Fr_q Re_q We	$Re_q > Re_{q,crit} = 10^3$ $We > We_{crit} = 10$
Wave overtopping	Gravity force Friction forces Surface tension	Fr_A, Fr_q Re_q We	$Re_q > Re_{q,crit} = 10^3$ $We > We_{crit} = 10$

With: $Fr_W = c/(g \cdot h)^{1/2}$; $Fr_A = v_A/(g \cdot h_A)^{1/2}$; $Fr_q = v_A/(2 \cdot g \cdot R_u)$; $Re_W = c \cdot h/\nu$; $Re_q = (R_u - R_C)^2/(\nu \cdot T)$; $We = v_A \cdot h_A \cdot \rho_W/\sigma_W$

From observations in prototype and scaled models, a methodology was derived to account for those differences without specifically defining which model and measurement effects contribute how much. These recommendations are given in subsections 5.7 for dikes, 6.3.6 for rubble slopes, and 7.3.6 and 7.3.7 for vertical walls, respectively.

4.9 Uncertainties in predictions

Sections 4.2 to 4.4 have proposed various models to predict wave overtopping of coastal structures. These models will now be discussed with regard to their uncertainties.

4.9.1 Empirical Models

It has been discussed in section 1.5.4 that the model uncertainty concept uses a mean factor of 1.0 and a Gaussian distribution around the mean prediction. The standard deviation is derived from the comparison of model data and the model prediction.

This has two implications for design: Probabilistic design values for all empirical models used in this manual describe the mean approach for all underlying data points. This means that, for normally distributed variables, about 50 % of the data points exceed the prediction by the model, and 50 % are below the predicted values. This value should be used if probabilistic design methods are used.

The deterministic design value for all models will be given as the mean value plus one standard deviation, which in general gives a safer approach, and takes into account that model uncertainty for wave overtopping is always significant.

4.9.2 Neural Network

When running the Neural Network model the user will be provided with wave overtopping ratios based on the CLASH database and the Neural Network prediction (Section 4.4). Together with these results the user will also obtain the uncertainties of the prediction through the 5 % and 95 % confidence intervals.

Assuming a normal distribution of the results will allow an estimate of the standard deviation of the overtopping ratio and hence the whole Gaussian distribution. Results from the Neural Network prediction can then be converted to the methodology referenced in Section 4.8 by providing all other confidence intervals and exceedance probabilities required there. Details will be given when test cases will be investigated.

4.9.3 CLASH database

The CLASH database is described in Section 4.5. It provides a large dataset of available model data on wave overtopping of coastal structures. It should be mentioned that the model and scale effects approach introduced in Section 4.8 has not been applied to the database. Whenever these data are used for prototype predictions the user will have to check whether any scaling correction procedure is needed.

With respect to uncertainties all model results will contain variations in the measured overtopping ratios. Most of these variations will result from measurement and model effects as discussed earlier. Since the database is no real model but an additional source of data information no model uncertainty can be applied.

4.10 Guidance on use of methods

This manual is accompanied by an overall Calculation Tool outlined in Appendix A. This tool includes the elements:

- **Empirical Calculator** programmed with the main empirical overtopping equations in Chapters 5, 6 and 7 (limited to those that can be described explicitly, that is without iteration).
- **PC-Overtopping**, which codes all the prediction methods presented in Chapter 5 for mean overtopping discharge for (generally shallow sloped) sea dikes, see section 4.3.
- **Neural Network** tool developed in the CLASH research project to calculate mean overtopping for many types of structures, see section 4.4.
- **CLASH database**, a listing of input parameters and mean overtopping discharge from each of approximately 10,000 physical model tests on both idealised (research) test structures, and site specific designs. These data can be sifted to identify test results that may apply for configurations close to the reader's, see section 4.5.

None of these methods give the universally 'best' results. The most reliable method to be used will depend on the type and complexity of the structures, and the closeness with which it conforms to simplifying assumptions used in previous model testing (on which all of the methods above are inherently based).

In selecting which method to use, or which set of results to prefer when using more than one method, the user will need to take account of the origins of each method. It may also be important in some circumstances to use an alternative method to give a check on a particular

set of calculations. To assist these judgements, a set of simple rules of thumb are given here, but as ever, these should not be treated as universal truths.

- For **simple vertical, composite, or battered walls** which conform closely to the idealisations in Chapter 7, the results of the Empirical Calculator are likely to be more reliable than the other methods as test data for these structure types do not feature strongly in the Database or Neural Network, and PC-Overtopping is not applicable.
- For **simple sloped dikes** with a single roughness, many test data have been used to develop the formulae in the Empirical Calculator, so this may be the most reliable, and simplest to use / check. For dikes with multiple slopes or roughness, PC-Overtopping is likely to be the most reliable, and easiest to use, although independent checking may be more complicated. The Database or Neural Network methods may become more reliable where the structure starts to include further elements.
- For **armoured slopes and mounds**, open mound structures that most closely conform to the simplifying models may best be described by the formulae in the Empirical Calculator. Structures of lower permeability may be modelled using PC-Overtopping. Mounds and slopes with crown walls may be best represented by application of the Database or Neural Network methods.
- For **unusual or complex structures with multiple elements**, mean overtopping discharge may be most reliably predicted by PC-Overtopping (if applicable) or by the Database or Neural Network methods.
- For structures that require use of the Neural Network method, it is possible that the use of many data for other configurations to develop a single Neural Network method may introduce some averaging. It may therefore be appropriate to check in the Database to see whether there are already test data close to the configuration being considered. This procedure may require some familiarity with manipulating these types of test data.

In almost all instances, the use of any of these methods will involve some degree of simplification of the true situation. The further that the structure or design (analysis) conditions depart from the idealised configurations tested to generate the methods/tools discussed, the wider will be the uncertainties. Where the importance is high of the assets being defended, and/or the uncertainties in using these methods are large, then the design solution may require use of site specific physical model tests, as discussed in section 4.6.